

## Microfluidic photonic crystal double heterostructures

Cameron L. C. Smith,<sup>a)</sup> Darran K. C. Wu, Michael W. Lee, Christelle Monat, Snjezana Tomljenovic-Hanic, Christian Grillet, and Benjamin J. Eggleton  
*Centre for Ultrahigh-Bandwidth Devices for Optical Systems (CUDOS), School of Physics, University of Sydney, Sydney, New South Wales 2006, Australia*

Darren Freeman, Yinlan Ruan,<sup>b)</sup> Steve Madden, and Barry Luther-Davies  
*Centre for Ultrahigh-Bandwidth Devices for Optical Systems (CUDOS), Laser Physics Centre, Australian National University, Canberra, Australian Capital Territory 0200, Australia*

Harald Giessen  
*4th Physics Institute, University of Stuttgart, D-70569 Stuttgart, Germany*

Yong-Hee Lee  
*Nanolaser Laboratory, Department of Physics, Korea Advanced Institute of Science and Technology (KAIST), Daejeon 305-701, Korea*

(Received 21 July 2007; accepted 28 August 2007; published online 17 September 2007)

We demonstrate postprocessed and reconfigurable photonic crystal double-heterostructure cavities via selective fluid infiltration. We experimentally investigate the microfluidic cavities via evanescent probing from a tapered fiber at telecommunication wavelengths. Fabry-Pérot fringes associated with modes of the induced cavity are in good agreement with the theory. We also demonstrate a cavity with quality factor  $Q=4300$ . Our defect-writing technique does not require nanometer-scale alterations in lattice geometry and may be undertaken at any time after photonic crystal waveguide fabrication. © 2007 American Institute of Physics. [DOI: 10.1063/1.2785988]

Research into optical microcavities based on photonic crystal slabs (PCSs) has attracted significant attention in the past several years. There are numerous applications for compact and low-loss microcavities, such as channel drop filters,<sup>1</sup> low-threshold lasers,<sup>2</sup> cavity quantum electrodynamics experiments,<sup>3</sup> optical switching,<sup>4</sup> and optical sensing.<sup>5</sup> The cavity design goals for these applications are high  $Q$  factors and small mode volumes.<sup>6</sup> Indeed, these two conditions can potentially give rise to a dramatic enhancement of light-matter interaction over a compact space, which is of particular relevance for optical switching and sensing.

The use of photonic crystal microcavities has widely exploited local alterations in the periodic geometry of PCS lattices. These structural modifications, referred to as “defects,” are performed during the fabrication step and typically result in the appearance of one or several cavity modes that are spatially confined within the defect. The defect is made, for instance, by omitting, shrinking, or enlarging one or more holes in the PCS.<sup>7</sup> More recently, “double heterostructures” have been achieved from a slight change of the PCS period over a finite area of the nominal PCS lattice.<sup>8</sup> However, the nanometer-scale precision required to realize sophisticated and optimized geometries eventually becomes a limiting factor in achieving high- $Q$  cavities, as pointed out by Asano *et al.*<sup>9</sup>

Recently, several groups have reported demonstrations of postprocessed PCS structures, granting them the flexibility to tune or reconfigure device properties to suit various applications at any time after the PCS is fabricated.<sup>10–13</sup> In particular, Intonti *et al.* introduced a “pixel by pixel” approach for writing and rewriting PCS defect structures via fluid

infiltration.<sup>12</sup> Theoretical results of Tomljenovic-Hanic *et al.* showed that high  $Q$ -factor cavities could be achieved in PCSs from fluid infiltration<sup>14</sup> by forming double-heterostructured geometries, providing an integrated optofluidic sensing architecture.

In this letter, we present experimental demonstrations of double heterostructure type microcavities formed within PCSs after their fabrication. Instead of exploiting a change of the PCS period, the double heterostructures are created by selectively fluid-filling a restricted region of the PCS using a micropipette. This approach offers a flexible way to write microcavities by choosing (i) the index of the infused liquid and (ii) the length and pattern of the infiltrated PCS area. In addition, the reversible nature enabled by fluid mobility offers a “rewrite” potential, paving the way for reconfigurable microphotonic devices<sup>15</sup> and sensing architectures.

Figure 1(a) illustrates the microfluidic-filled double-heterostructure waveguide cavity of the present study. The initial PCS structure is a W1 waveguide that results from the omission of a single row of air holes along the  $\Gamma$ - $K$  direction of a triangular photonic crystal lattice. The central section of the waveguide, denoted by the lighter circles, is filled with a liquid across its length. The fluid-filled holes present a dif-

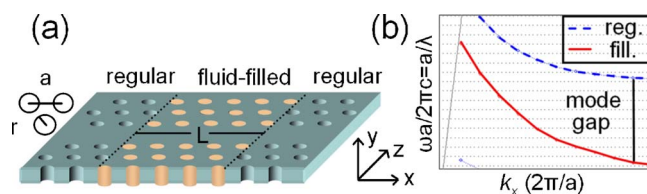


FIG. 1. (Color online) (a) Double-heterostructure microcavity with lattice period  $a$  and hole radius  $r$ . Fluid-filled holes have a refractive index  $n = 1.4$ ; the rest are  $n = 1.0$ . Refractive index of the slab is  $n = 2.68$ . (b) Dispersion relation for regular (dashed) and fluid-filled (solid) photonic crystal waveguides. The difference between the curves is labeled mode gap.

<sup>a)</sup>Electronic mail: csmith@physics.usyd.edu.au

<sup>b)</sup>Present address: Centre of Expertise in Photonics, School of Chemistry & Physics, University of Adelaide, Adelaide, 5005, Australia.

ferent refractive index  $n_{\text{holes}}$  than those enclosed in the surrounding nominal PC lattice, with the different PCS sections forming a double heterostructure.

Figure 1(b) summarizes the mechanism of the double-heterostructure cavity, which can be understood qualitatively by comparison of the dispersion curves of two W1 waveguides with different  $n_{\text{holes}}$ .<sup>8</sup> As a result of the  $n_{\text{holes}}$  increase (here from 1 to 1.4), the fundamental guided mode of the waveguide is shifted towards lower frequencies. This creates a “mode gap” between the fundamental mode of the filled and unfilled waveguides. Consequently, a waveguide mode that is excited in the fluid-filled section with a frequency lying in this mode-gap window cannot propagate any further in the surrounding unfilled waveguide area. Instead, it remains localized within the fluid-filled section, decaying evanescently in the surrounding unfilled region.<sup>14</sup>

The experimental PCS structure is made from chalcogenide glass (“AMTIR-1”  $\text{Ge}_{33}\text{As}_{12}\text{Se}_{55}$ ), having a refractive index  $n_{\text{slab}}=2.68$ . The lattice constant is  $a=550$  nm, slab thickness  $T=300$  nm, and hole radius  $r=190$  nm. The photonic bandgap of this structure spans optical telecommunication frequencies. The entire PCS structure is 40 periods in the  $x$  direction and 19 periods in the  $z$  direction. To create the cavity, we introduce an index-matching fluid of refractive index  $n=1.4$  selectively into some air holes of the PCS. We use a tapered glass micropipette with  $2\ \mu\text{m}$  tip diameter, which is mounted onto a micromechanical stage. The tip is inserted within a large meniscus of the filling fluid. As the tip is withdrawn from the meniscus, droplets of the fluid remain along its length due to surface tension and the hydrophilic nature of the glass. These droplets are then deposited in close proximity to the PCS structure under a high magnification ( $100\times$ ) microscope. Finally, by careful manipulation of the micropipette, a droplet of choice is drawn along the photonic crystal to create the double heterostructure.

We investigate the fluid-filled double heterostructures via evanescent probing.<sup>16</sup> A silica fiber with its diameter reduced to  $0.8\ \mu\text{m}$  for a  $2\ \text{mm}$  length is brought into close proximity with the cavity. Due to the reduction in size, the evanescent field extends significantly beyond the tapered fiber boundary, allowing it to interact with the waveguide.

Evanescent probing provides a method to check that the fluid penetrates the pores of the photonic crystal and does not form an excess fluid “layer.” This is evident when an overabundance of fluid is drawn along the waveguide and unwanted meniscus forms; the tapered fiber suffers significant broadband losses. Typically the fluid infiltration experiments described further below did not result in observable loss.

The first investigated PCS double heterostructure has a fluid-filled section of  $9.8\ \mu\text{m}$  length, as shown in Fig. 2(a). Figures 2(b) and 2(c) show the experimental transmission through the tapered fiber as it is evanescently coupled to the waveguide, before and after the liquid infiltration. For both measurements, the tapered optical fiber is in contact with the structure, over a length estimated to be  $15\ \mu\text{m}$ . Without the liquid, a single dip is obtained at  $1570\ \text{nm}$ , which corresponds to the coupling into the fundamental mode of the waveguide.<sup>17</sup> After the liquid infiltration, the spectrum displays additional features at slightly longer wavelengths to the reference fundamental. We attribute these dips to Fabry-Pérot (FP) resonances as the fundamental mode of the fluid-filled waveguide [solid curve of Fig. 1(b)] undergoes multiple reflections at the discontinuities between the different

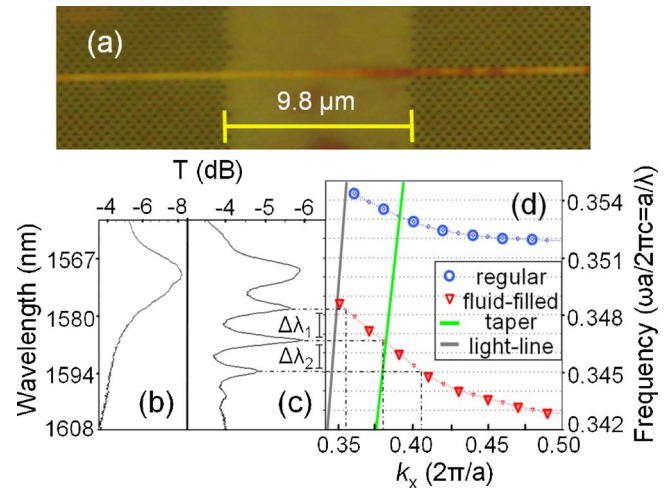


FIG. 2. (Color online) (a) Microscope image of W1 PCS structure with a  $9.8\ \mu\text{m}$  fluid-filled section. [(b) and (c)] Experimental transmission from the taper when it is coupled to the W1 PCS, (b) before and (c) after the fluid filling. (d) Dispersion curves of the silica taper and the W1 PCS, both fluid filled (triangles) and unfilled with fluid (circles), as calculated separately using a 3D plane-wave method. Used wavevector  $k_x$  is taken along the waveguide direction. Where the taper curve intersects with W1 PCS curves, phase matching (coupling) occurs. Trace (c) displays additional FP resonances, which can be related to the calculated dispersion curve of the fluid-filled W1 PCS.

PCS sections, which act as effective mirrors in the mode-gap window.

The number of FP peaks that are observed experimentally is limited to 3–4 over the predicted mode-gap window. Note that the coupling strength of the FP peaks with the taper is at a maximum for the  $1586.5\ \text{nm}$  feature and decreases for the other peaks on both sides of this wavelength due to an increased phase mismatch between the fiber and the cavity modes.<sup>16</sup> Also, one can notice a larger linewidth of the shorter wavelength dip at  $1570\ \text{nm}$ , which corresponds with coupling to the fundamental mode of the regular waveguide where the tapered fiber interacts with it outside the fluid-filled section. The wavelength of the FP resonances should roughly meet the following condition:

$$2k_x L = 2\pi p, \quad (1)$$

which relates the wavevectors  $k_x$  of the FP resonances to the fluid-filled cavity length  $L$  through an integer  $p$ .<sup>18,19</sup>

The wavelengths of the experimental dips have been superimposed onto the dispersion curve of the infiltrated waveguide mode of Fig. 2(d), calculated using a three-dimensional (3D) plane-wave method with a supercell approach (RSoft’s BANDSOLVE) using the PCS parameters mentioned earlier. Their corresponding wavevectors, as extracted from the dispersion curve, display a nearly equal separation that is roughly  $\pi/L$ , in close agreement with Eq. (1). At the same time, the experimental free spectral range between the resonances becomes smaller as  $\lambda$  becomes longer ( $\Delta\lambda_1=7.65\ \text{nm}$  and  $\Delta\lambda_2=7.45\ \text{nm}$ ). This is consistent with the dispersive behavior of the infiltrated waveguide mode that presents a decrease in group velocity at lower energy. Indeed, the group velocity can be related to the wavelength separation  $\Delta\lambda$  between the FP peaks, according to  $V_g=2Lc\Delta\lambda/\lambda^2$ . This relation produces an estimate of the group velocity ranging between  $c/16.8$  and  $c/17.2$ , in close agreement with the dispersion displayed in Fig. 2(d). The slight discrepancy between experimental and theoretical data

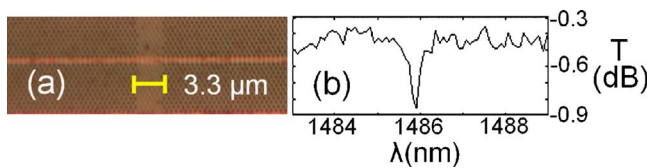


FIG. 3. (Color online) (a) Image of W1 PCS structure with a  $3.3 \mu\text{m}$  fluid-filled section. (b) Corresponding experimental transmission when probed by evanescent coupling displaying high- $Q$  ( $Q=4300$ ) resonance.

(especially for the fundamental mode resonance frequency) is attributed to the simplification of our modeling, which is based on the assumption that coupling between the cavity and the taper is weak. This is not the case due to the direct contact between the taper and the waveguide.

Second, we investigate a fluid-filled cavity with length  $L=3.3 \mu\text{m}$ , as shown in Fig. 3(a). Evanescent probing of this structure provides a transmission spectrum with a distinct and narrow feature, as displayed in Fig. 3(b). The corresponding net  $Q$ -factor  $Q_T$  of the dip measured experimentally encompasses all the different decay channels available to the photons in the system, given by

$$\frac{1}{Q_T} = \frac{1}{Q_0} + \frac{1}{Q_{\text{fiber}}} + \frac{1}{Q_{\text{parasitic}}}, \quad (2)$$

where  $Q_0$  is the intrinsic  $Q$ -factor of the cavity,  $Q_{\text{fiber}}$  is the coupling between the cavity and the taper, and  $Q_{\text{parasitic}}$  is the parasitic losses associated with any significant perturbation of the cavity mode field.<sup>10</sup> Our measured quality factor is  $Q_T=4300$ , with a transmittance of 90%.

Apart from the reconfigurable photonic device application offered by this approach, potential can be found for optical sensors.<sup>5,15</sup> The sensor based PCS designs that have been proposed thus far typically require an alignment between the defect and infiltrated area. In addition, high  $Q$ -factors of the optical modes involved in the sensing scheme are typically degraded by the fluid infiltration step. Here, these problems are solved because the initial structure presents no cavity mode in the absence of fluid while the fluid itself potentially generates the high- $Q$  resonances. This architecture could be readily exploited to create a series of multiple and parallel integrated sensors, each of them having, for instance, a different infiltrated width and addressing a different substance.

In conclusion, we demonstrate a postprocessing capability to form photonic crystal double heterostructures at telecommunication wavelengths. These are introduced within a PCS by selectively filling a small region of air holes using a micropipette, whose size can be readily rewritten. Initial experiments observed cavity characteristics with a measured  $Q$ -factor of  $Q=4300$ .

The support of the Australian Research Council through its Federation Fellow, Centres of Excellence, Denison Foundation, and Discovery Grant programs is gratefully acknowledged.

<sup>1</sup>B. S. Song, S. Noda, and T. Asano, *Science* **300**, 1537 (2003).

<sup>2</sup>H. G. Park, J. K. Hwang, J. Huh, H. Y. Ryu, Y. H. Lee, and J. S. Kim, *Appl. Phys. Lett.* **79**, 3032 (2001).

<sup>3</sup>D. Englund, D. Fattal, E. Waks, G. Solomon, B. Zhang, T. Nakaoka, Y. Arakawa, Y. Yamamoto, and J. Vučković, *Phys. Rev. Lett.* **95**, 013904 (2005).

<sup>4</sup>T. Tanabe, M. Notomi, S. Mitsugi, A. Shinya, and E. Kuramochi, *Opt. Lett.* **30**, 2575 (2005).

<sup>5</sup>M. Loncar, A. Scherer, and Y. M. Qiu, *Appl. Phys. Lett.* **82**, 4648 (2003).

<sup>6</sup>K. J. Vahala, *Nature (London)* **424**, 839 (2003).

<sup>7</sup>Y. Akahane, T. Asano, B. S. Song, and S. Noda, *Nature (London)* **425**, 944 (2003).

<sup>8</sup>B. S. Song, S. Noda, T. Asano, and Y. Akahane, *Nat. Mater.* **4**, 207 (2005).

<sup>9</sup>T. Asano, B. S. Song, and S. Noda, *Opt. Express* **14**, 1996 (2006).

<sup>10</sup>C. Grillet, C. Monat, C. L. C. Smith, B. J. Eggleton, D. J. Moss, S. Frederick, D. Dalacu, P. J. Poole, J. Lapointe, G. Aers, and R. L. Williams, *Opt. Express* **15**, 1267 (2007).

<sup>11</sup>M. W. Lee, C. Grillet, C. L. C. Smith, D. J. Moss, B. J. Eggleton, D. Freeman, B. Luther-Davies, S. Madden, A. Rode, Y. Ruan, and Y.-H. Lee, *Opt. Express* **15**, 1277 (2007).

<sup>12</sup>F. Intonti, S. Vignolini, V. Turck, M. Colocci, P. Bettotti, L. Pavesi, S. L. Schweizer, R. Wehrspohn, and D. Wiersma, *Appl. Phys. Lett.* **89**, 211117 (2006).

<sup>13</sup>D. Erickson, T. Rockwood, T. Emery, A. Scherer, and D. Psaltis, *Opt. Lett.* **31**, 59 (2006).

<sup>14</sup>S. Tomljenovic-Hanic, C. M. de Sterke, and M. J. Steel, *Opt. Express* **14**, 12451 (2006).

<sup>15</sup>C. Monat, P. Domachuk, and B. J. Eggleton, *Nat. Photonics* **1**, 106 (2007).

<sup>16</sup>P. E. Barclay, K. Srinivasan, M. Borselli, and O. Painter, *Electron. Lett.* **39**, 842 (2003).

<sup>17</sup>C. Grillet, C. Smith, D. Freeman, S. Madden, B. Luther-Davis, E. C. Mägi, D. J. Moss, and B. J. Eggleton, *Opt. Express* **14**, 1070 (2006).

<sup>18</sup>X. Letartre, C. Seassal, C. Grillet, P. Rojo-Romeo, P. Viktorovitch, M. L. d'Yerville, D. Cassagne, and C. Jouanin, *Appl. Phys. Lett.* **79**, 2312 (2001).

<sup>19</sup>M. Notomi, K. Yamada, A. Shinya, J. Takahashi, C. Takahashi, and I. Yokohama, *Phys. Rev. Lett.* **87**, 253902 (2001).